

Formal kinetic evaluation of reactions with partial diffusion control

H.J. Flammersheim^{a,*}, J. Opfermann^b

^aFriedrich-Schiller-Universität Jena, Chem. Geowiss. Fak., Inst. für Phys. Chem., Lessingstr. 10, 07743 Jena, Germany

^bNETZSCH-Gerätebau GmbH, Wittelsbacherstraße 42, 95100 Selb, Germany

Received 4 May 1999; received in revised form 7 June 1999; accepted 7 June 1999

Abstract

The use of non-linear regression for a series of measurements with different heating rates or different reaction temperatures (multivariate non-linear regression) allows the reliable formal kinetic evaluation of reactions. As a result, an optimum data reduction is achieved and the practitioner can predict the reaction behaviour for any reaction conditions. Even reactions with partial diffusion control can now be investigated. In this paper we demonstrate this for DSC measurements of an epoxy resin curing reaction. The only additional requirement is the measurement of a glass transition temperature T_g as function of conversion α . © 1999 Elsevier Science B.V. All rights reserved.

Keywords: Epoxy curing; Kinetics; Diffusion control; DSC; Temperature modulated DSC

1. Introduction

The detailed mechanisms of many reactions, important for technical applications, are only partially known. To make matters worse, the exact composition of the reacting system is not known or not published for reasons of protective rights. In such cases a kinetic analysis of the reaction in the physical–chemical sense is not possible, even if there is enough time for such studies.

But the practitioner needs a useful and quickly accessible “reaction model”, which on one hand adequately describes the course of the reaction and on the other allows reliable predictions for any temperature–time-conditions. The form of this reaction model (overall rate law, combination of “elementary reactions”) is unimportant. The kinetic evaluation of

some technically essential polymerization reactions is additionally complicated by the fact that for some reaction conditions (low heating rates, annealing periods) the glass temperature of the polymer increases faster than the program temperature. After the partial or complete freezing of the reaction mixture the reaction is no longer controlled by the kinetics of the chemical reaction, but by diffusion processes. Finally, if the program temperature exceeds the maximum glass transition temperature, one enters again the realm of chemical reaction control.

In describing the formal kinetics of complex reactions we can distinguish between three principle procedures:

In the past many reactions were described by empirically found overall rate laws or by rate laws which were derived from a postulated and sometimes oversimplified reaction mechanism. Frequently, the fit of the experimental data was

*Corresponding author. Fax: +49-03641-948302
E-mail address: c7flha@uni-jena.de (H.J. Flammersheim)

improved by introducing additional parameters and/or the restriction to limited conversion ranges. A typical example is the so-called ‘Kamal’-equation [1,2] which is often used for the polymerization reaction of epoxides:

$$\frac{d\alpha}{dt} = \left(k_1 + k_2 \alpha^{m(T)} \right) \cdot (1 - \alpha)^{n(T)}.$$

In this equation the original integer reaction orders n and m are replaced by freely selectable, broken and temperature-dependent fit parameters.

Using modern methods of data acquisition and evaluation two other procedures offer clear advantages.

The Ozawa–Flynn–Wall method [3,4] allows the model-free and conversion-dependent estimation of the overall activation energy. Assuming an additive superposition of the contributions of the individual partial reactions as a function of conversion, predictions for other reaction conditions can also be made in many cases, according to Vyazovkin [5].

According to Opfermann [6] the overall process is described by multi-step processes with constant activation parameters. The single steps can be independent, parallel, competitive or consecutive. This is the more advantageous procedure, being generally applicable, even for reactions with independent competitive reactions and such with partial diffusion control. An interpretation of the single steps and their parameters should be done very cautiously, if at all. In this paper we investigate the curing reaction of a commercial epoxy resin. The only disadvantage for the time being is the restriction to systems of equal initial composition.

The concept of (partial) diffusion control for epoxy curing reactions is already well documented by means of very different approaches [7–9]. Using the temperature-modulated DSC [10] a technique is available that allows the detection of the temperature range of a possible diffusion control without any doubt. Besides, this technique offers the possibility to obtain the T_g conversion curve quickly and sufficiently reliably. This is a necessary precondition for the consideration of the diffusion control.

2. Experimental

A commercial epoxy (2,2',6,6'-tetrabrom-bisphenol-A-diglycidylether, RUETAPOX VE 3579, in the glassy amorphous state, $T_g = 25^\circ\text{C}$) was used in combination with 5% of a self-prepared thermal latent accelerator ($\text{Zn}(\text{OCN})_2$ (1MeImid)₂, crystalline powder, release of the 1-methylimidazol above the melting point at about 70°C). The reaction mixture which results during mortaring both solid components can be stored nearly infinitely below 25°C . Standard pans of aluminium foil were used for sample preparation. The sample masses were 5–20 mg, depending on the program heating rate.

Most of the measurements were obtained with an MDSC 2920 (TA Instruments) with RCS-cooling. The modulation periods were 60 and 100 s, the modulation amplitudes from ± 0.15 up to ± 1.0 K (depending on the heating rate). Supplementary measurements were carried out using the DSC 2 and DSC 7 (Perkin Elmer). As usual all instruments were calibrated in the temperature range from -30°C up to 250°C regarding base line, temperature (water, indium and tin), heat (indium) and heat flow rate (sapphire).

The original non-reversing heat flow rate curves could only be used for the kinetic analysis after several corrections had been done:

(1) The real heating rates (underlying heating rates) were a factor of 0.971 lower than the program heating rates (0.1, 0.25, 0.5, 0.75, 1.0, 1.5, 2.0, 3.5 and 5.0 K/min^{-1}). Besides, the heat flow rate calibration of MDSC 2920 is somewhat temperature-dependent. The available software version of the manufacturer allows only a constant, average correction for the relationship between the literature and measured value. Therefore, this correction was not made. Instead, the measured heat capacities were corrected later on with a temperature-dependent function, which was calculated from the deviation between the literature and measured c_p -values for sapphire. The corrected reversing and non-reversing heat flow rate curves were recalculated as follows:

- (a) reversing heat flow rate curve = corrected c_p value * real heating rate,
- (b) non-reversing heat flow rate curve = total heat flow rate curve – reversing heat flow rate curve.

(2) In temperature ranges, that correspond to the decomposition of the initiator or the highest heat flow rate changes during the reaction, minor disturbances in the reversing signal are observed, that disappear only at heating rates $<1 \text{ K min}^{-1}$. The first disturbance does not have any influence on the evaluation, as the reaction starts with a distinct rate only above 70°C . The correction of the second effect is simple. As heat capacity function and reversing signal are smooth, steady and nearly linear functions of the temperature, a linear extrapolation from temperature ranges without interruption into the interrupted ranges is possible.

(3) The non-reversing curve of a completely reacted sample should not show a signal over the whole temperature range. In spite of careful baseline calibration this requirement was not sufficiently fulfilled in our measurements (compare Fig. 4). This is clearly verified by repeated measurements with samples, that – to be on the safe side – were additionally tempered at 180°C for another 10 h. Typical values for the differences of the heat flow rate signals between 0°C and 200°C were found in the range $\pm 0.05 \text{ W g}^{-1}$. In our case this drift is extremely disturbing, because the reaction during the first run is not yet completely finished at the maximum allowed end temperature of 200°C . Hence, it cannot be decided which portion of the signal at 200°C means drift or reaction. All attempts to obtain reproducibly drift-free curves or at least such with a constant drift failed up to now. The observed drift did not depend on sample mass, heating rate, period and amplitude of the temperature modulation. Possibly, a minor parasitic heat transfer between sample and instrument, depending on the individual sample, (eventually an exemplary feature of the available measuring head) plays a decisive part. This assumption is supported by the observation that multiple runs with one and the same completely reacted sample yield practically identical results for the heat capacity function and the reversing and non-reversing heat flow rate curves. Our used correction procedure is derived from and justified by this observation. The curve of the repeated run should include all non-desired instrumental influences as a sum. Besides the drift, this is valid also for a small curvature of the baseline. As the first and second run are falsified in the same way by these influences, one obtains the real reaction signal as a difference between the (corrected) non-reversing curves of the first and second

run. Nevertheless, the remaining uncertainty regarding this correction decisively influences the reliability of the respective data set for the latter kinetic analysis.

3. Results and discussion

The reaction heat was obtained as $260 \pm 10 \text{ J g}^{-1}$. Figs. 1–3 show the heat flow rate curves at a very slow heating rate (0.25 K min^{-1}), the heat capacity measurements at different heating rates and the course of the isothermal curing at 95°C . Three characteristics of the investigated reaction can be clearly deduced from these figures. They have to be considered in the kinetic analysis:

(1) Apart from the mentioned uncertainty regarding the slope of the respective curve the reproducibility of

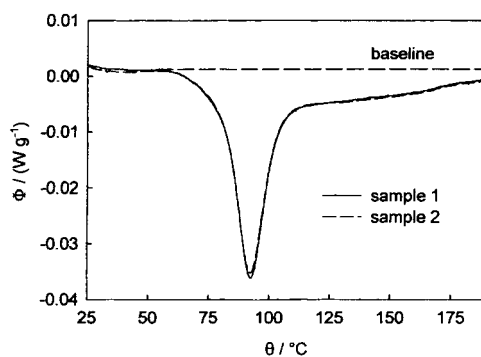


Fig. 1. Non-reversing heat flow rates for the curing of two samples at $\beta = 0.243 \text{ K min}^{-1}$, sample masses 21.17 and 21.91 mg.

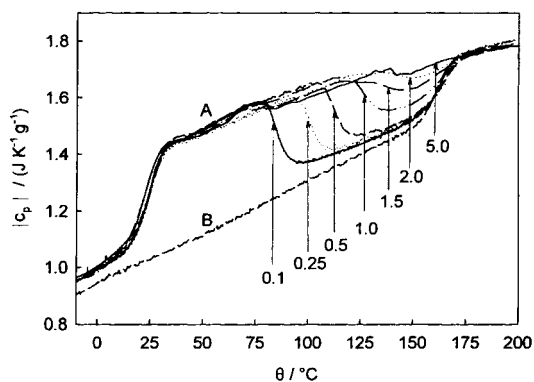


Fig. 2. (A) Heat capacity curves of the first runs at different heating rates (numbers at the arrows). (B) Heat capacity curve of the reaction product, calculated from all second runs.

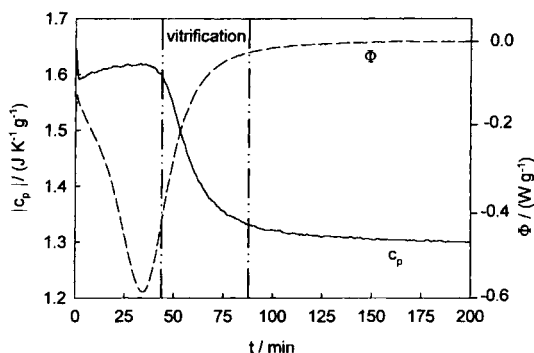


Fig. 3. Non-reversing heat flow rate and heat capacity during the isothermal reaction at 95°C, sample mass 8.2 mg. The vertical lines mark the vitrification range.

the measurements is excellent (Fig. 1). T_g of the basic resin is $25 \pm 1^\circ\text{C}$, the one of the reacted system $165 \pm 2^\circ\text{C}$. The reaction starts with a detectable rate at about $70\text{--}80^\circ\text{C}$, coupled to the decomposition of the finely dispersed latent accelerator. In the first reaction stage the sample temperature is clearly higher than the glass temperature of the reacting system at all used heating rates. The observed reaction rate is only dependent on the rate of the chemical reaction (kinetically controlled). However, at all heating rates the glass temperature increases faster than the program temperature. The system vitrifies partially (arrows in Fig. 2, see also Fig. 8). The degree of vitrification at this temperature is given by the ratio of the respective step height to the maximum step width of the final product. In the temperature range between vitrification and devitrification at about 165°C the reaction is more or less diffusion-controlled.

(2) Fig. 3 proves definitely that one or several reaction steps are autocatalytical. The range of the isothermal vitrification of the system is clearly displayed by the decrease of the heat capacity in this figure (between the both vertical lines). However, it does not manifest itself – as often stated in literature – by a noticeable sudden decrease of the reaction rate in the heat flow rate curve.

(3) Fig. 1 shows that the reaction is not yet finished at 200°C even at very low heating rates. The heat flow rate is still different from zero. From this follows the selection of the peak baseline. Its constant level is given by the signal at the beginning of the reaction. An upper temperature limit of $190\text{--}200^\circ\text{C}$ must not be exceeded, in order to avoid incipient decomposition

reactions of the product. This is sensitively indicated by the decrease of the maximum glass temperature.

Taking into account these observations, the kinetic model should be as simple as possible. Only then the parameters of the individual steps can be significantly obtained. If diffusion hindrances must be additionally considered, the Rabinowitch equation can be used for the overall rate constant k [11]:

$$\frac{1}{k} = \frac{1}{k_{\text{diff}}} + \frac{1}{k_{\text{chem}}}$$

As usual the temperature dependence of k_{chem} is calculated by the Arrhenius equation. The concrete form of the temperature function for k_{diff} is absolutely unimportant. However, it should be such that the experimental input necessary for the calculation of the selected function is the easily accessible glass temperature. Therefore, most authors use any modified equations of the WLF type. We use a form as proposed by Wise et al. [12]:

$$k_{\text{diff},T} = k_{\text{diff}} \cdot e^{(C_1 \cdot (T - T_g)) / (C_2 + T - T_g)}$$

The magnitude of k_{diff} can be estimated using a relation as given by Smoluchowski [13]:

$$k_{\text{diff}} = 4\pi \cdot N_A \cdot r \cdot D$$

N_A is the Avogadro constant. Wise et al. [12] use 0.5 nm for the collision radius r . The diffusion coefficient D used by the same authors ($10^{-20} \text{ m}^2 \text{ s}^{-1}$) for the diffusion of small molecules in a polymer matrix is only a rough approximation for the investigated reaction system. Therefore, the value of k_{diff} given by Wise et al. for the glass temperature ($3.8 \times 10^{-5} \text{ mol}^{-1} \text{ m}^3 \text{ s}^{-1}$) is only a usable start value for the optimization calculations. Frequently used values for the WLF parameter C_1 and C_2 are 40 and 52 K.

The kinetic modelling by means of multivariate non-linear regression was carried out using the Software "NETZSCH Thermokinetics" (NETZSCH-Gerätebau GmbH). The new version of this commercial software was extended by the software producer in such a way, that as an option the diffusion control is admitted for all reaction steps. For the fit of the reaction curves to a kinetic model we postulate that k_{diff} may be different for each diffusion-controlled reaction step, but C_1 and C_2 must be global. That means, they must be valid for all reaction steps. With this restriction k_{diff} , C_1 and C_2 can be handled as freely variable parameters for the

model. In order to realize a partial diffusion control the user must provide a reliable function $T_g(\alpha)$. The “activation parameters” (the term “process parameters” would rather emphasize the formal kinetic evaluation) of the single reactions of the selected model are strongly influenced by more or less reliably measured glass transition temperature T_g as function of conversion. Therefore, a lot of care should be taken in the determination of the $T_g(\alpha)$ -function. It includes the following steps:

1. Complete curing of a sample and calculation of $\Delta_r H$ and $\alpha = f(T)$.
2. Partial curing of a number of further samples up to temperatures that correspond to the desired conversion degrees. Freezing of the reaction by quenching the samples down to ambient temperature.
3. Post-curing of these samples, using the temperature-modulated mode of the DSC. Fig. 4 shows two examples. T_g (53°C and 98°C for the samples 1 and 2) is obtained from the reversing curves (at the bottom in the figure), the residual heat from the non-reversing curves (at the top). From the latter value follows α at the start of the reaction (0.248 and 0.598 for the two samples). The post-curing starts in the temperature range of the glass transition.
4. Calculation of the function $T_g = f(\alpha)$ in the kinetics software, using the following equation, [14]:

$$T_g(\alpha) = T_g(0) \cdot \exp\left(\frac{g_1 \cdot \alpha}{g_2 - \alpha}\right).$$

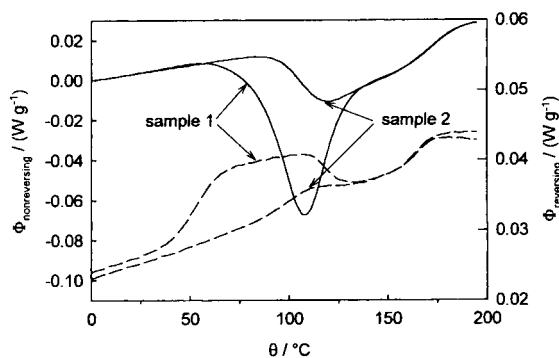


Fig. 4. Non-reversing (solid lines) and reversing (dashed lines) heat flow rates for the post-curing of two samples $\beta = 1.458 \text{ K min}^{-1}$, sample masses about 9 mg.

Table 1

Experimental and fitted glass transition temperatures vs. degree of reaction

Degree of reaction	T_g (°C) Measured	Calculated
0.000	25.0	23.1
0.248	53.0	51.8
0.310	58.0	59.6
0.379	65.0	68.6
0.455	78.0	78.9
0.598	98.0	99.6
0.688	116.0	113.5
0.763	128.0	125.7
0.832	140.0	137.3
1.000	165.0	167.8

Table 1 contains the measured and the regression T_g values (fit parameters $T_g(0) = 296.26 \text{ K}$, $g_1 = 4.48$ and $g_2 = 12.26$) as function of the conversion degree. Fig. 5 shows the good fit.

Two data sets were available for the kinetic analysis, each with 8 different heating rates between 0.25 and 5 K min^{-1} . The model calculations with these two data sets were carried out separately because the present software version only allows 8 scans to be loaded in. After loading in the data and before starting the kinetic evaluation, each curve is desmeared, temperature-corrected with regard to slight self-heating [15] and smoothed if required. The most simple model that produces a practically perfect fit of the scans for both data sets (correlation coefficients >0.999) corresponds to a process with two consecutive partial steps.

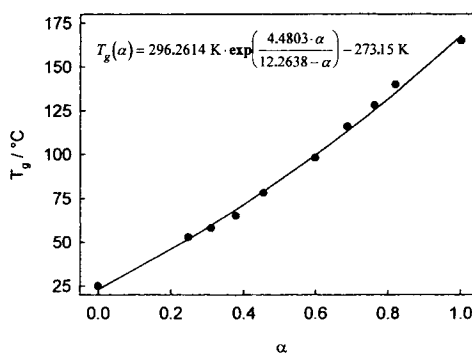
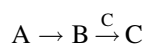


Fig. 5. Glass transition temperature vs. degree of reaction: (●) experimental values; (—) regression line.

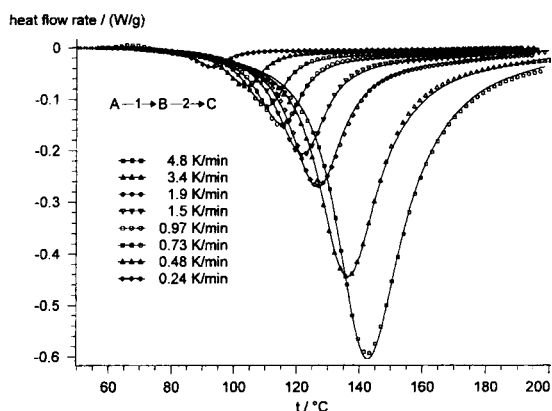


Fig. 6. Comparison between measured (symbols) and calculated (solid lines) DSC curves.

The comparison between measured and calculated curves for one data set is shown in Fig. 6. If in the kinetic calculation the “reaction orders” for the two subsequent reactions are also optimized, then one obtains values very close to $n_1 = 1$ and $n_2 = 2$. Therefore, they were kept constant at $n_1 = 1$ and $n_2 = 2$ for all further calculations. The second reaction step is auto-catalyzed by the reaction partner “C”. The “NETZSCH Thermokinetics” software takes into account the auto-catalysis for the second reaction step by the following differential equation [16]:

$$-\frac{dc_B}{dt} = A_2 \cdot e^{-E_{A,2}/RT} \cdot c_B^{n_2} \cdot (1 + K_{cat} \cdot c_C).$$

Only this step 2 is influenced by the diffusion. If as a trial the diffusion control is not used for this step, no acceptable fit is reached. The WLF parameter C_2 was set to a constant value of 50 K. Then, the resulting values for k_{diff} (4.3×10^{-5} up to $6.9 \times 10^{-5} \text{ mol}^{-1} \text{ m}^3 \text{ s}^{-1}$) approach the value mentioned by Wise et al. [12]. The model parameters for both data sets are summarized in Table 2; for the interpretation the following points are important:

(a) Even very careful measurements are never free from errors (heat flow rate curves, $T_g = f(\alpha)$). The existence of momentary disturbances influences all subsequent points of the model calculations. These aspects and the high correlation between activation energies and pre-exponential factors result in case of models with several partial steps very fast in the fact that the standard errors of the single parameters are significantly higher in reality than those obtained from

Table 2

Regression parameters and statistics for the two data sets

Parameter	Data set 1	Data set 2
$\lg(A_1/\text{s}^{-1})$	6.152	5.764
$E_{A,1}$ (kJ mol ⁻¹)	67.85	64.79
$\lg(A_2/\text{s}^{-1})$	8.178	9.0553
$E_{A,2}$ (kJ mol ⁻¹)	80.48	87.26
$\lg K_{cat,2}$	0.7833	0.7263
$\lg(K_{diffusion, 2}/\text{mol}^{-1} \text{ m}^3 \text{ s}^{-1})$	-4.3697	-4.1584
C_1 (K)	13.34	12.09
C_2 (K)	50	50
Fraction of consecutive reaction	0.2563	0.2326
Weighted least squares	0.090	0.094
Mean of residues	0.006	0.0061
Correlation coefficient	0.9996	0.9995

the parameter estimation according to the usual statistical procedure. Therefore, for both data sets the standard errors are not indicated – a more realistic image of the variation range can be obtained by the comparison of corresponding parameters in Table 2. On first examination the variation range seems to be considerable. But if, on the other hand, each data set is fitted with the parameter set of the other data set, the fit has practically the same perfect quality. In other words, there are a great number of parameter sets that describe the imperfect measurements practically just as well.

(b) It must be emphasized, that if other information is missing a mechanistic interpretation of both the model type and the model parameters is forbidden. However, this is indeed not the purpose of formal kinetic evaluations.

(c) The use of the obtained results becomes evident at quite different aspects. Each of both the parameter sets enables exact predictions of the reaction course for any temperature-time conditions. For example, Fig. 7 shows the predicted isothermal reaction curves at 110°C and 140°C. Both parameter sets produce curves which differ only within the line width. Also the agreement with the experiment is excellent (the heat flow rates of isothermal measurements are erroneous during the first 30–40 s). Furthermore, the final reaction degrees are clearly lower than 1 at low temperatures due to the freezing of the reaction after finite times. The corresponding values are correctly predicted for some temperatures (110°C: calculated 0.58, found 0.57 and 0.61; 140°C: calculated 0.80,

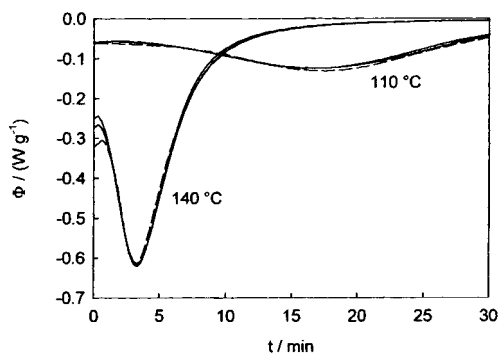


Fig. 7. Comparison between calculated (solid lines) and measured (dashed lines) isothermal curves, using the two slightly different parameter sets of Table 2, sample masses about 6 mg.

found 0.79 and 0.79; 170 °C: calculated 0.94, found 0.93 and 0.94).

A convincing argument for the validity of the selected model is finally given in Fig. 8. The course of the heat capacity function that can be directly accessed by experiment and is known already from Fig. 2 runs completely parallel to the increase of the glass temperature calculated by means of the model. This is valid both for the freezing at about 100 °C and the slow defreezing starting at about 130 °C. Here, the increase of T_g follows the programmed temperature exactly! This temperature range becomes larger using even lower heating rates and lower using higher heating rates. At heating rates $>1 \text{ K min}^{-1}$ T_g permanently lags behind the program temperature, as the diffusion hindrances due to partial freezing become more and more unimportant.

4. Conclusions

The use of modern kinetic evaluation methods for complex reactions allows the selection of the simplest and most appropriate formal-kinetic model and the reliable estimation of its activation parameters. This is valid also in the case of partially diffusion-controlled reactions. In this case, the Rabinowitch equation enables the possibility to consider both chemical and diffusion reaction control. The success and the reliability of such evaluations is determined by the correctness of the baseline and a well-known T_g -conversion curve. Both sets of information are obtained from MDSC measurements. The mentioned corrections of the raw signal should be increasingly unnecessary, resulting from better measuring devices. Investigating complex reactions, one typically sees as a result that a number of parameter sets describe the reaction behaviour of the system nearly just as well. This follows from the high correlation between pre-exponential factor and activation energy and the unavoidable measuring errors. For the practitioner this fact has no consequences because the predictions for any temperature–time reaction conditions are practically equal for all parameter sets.

Acknowledgements

We thank Mr. M. Döring (Inst. für Anorganische und Analytische Chemie, FSU Jena) for providing the substances. HJF thanks TA Instruments GmbH (Germany) for allowing to use temporarily an MDSC 2920.

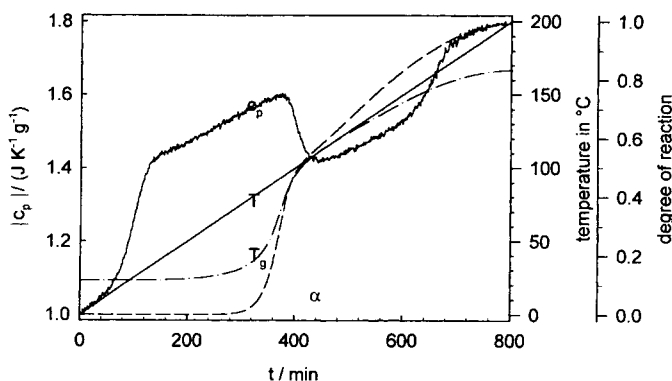


Fig. 8. Heat capacity, degree of reaction, program temperature and glass transition temperature as function of reaction time.

References

- [1] S. Sourour, M.R. Kamal, *Thermochim. Acta* 14 (1976) 41.
- [2] G. Höhne, W. Hemminger, H.J. Flammersheim, *Differential Scanning Calorimetry*, Springer, 1996, pp.139–153.
- [3] T. Ozawa, *Bull. Chem. Soc. Japan* 38 (1965) 1881.
- [4] J. Flynn, L.A. Wall, *Polym. Lett.* 4 (1966) 232.
- [5] S. Vyazovkin, *Int. J. Chem. Kinet.* 28 (1996) 95.
- [6] J. Opfermann, *J. Therm. Anal. Cal.*, in press.
- [7] J.M. Barton, *Polymer* 21 (1980) 603.
- [8] F.G.A.E. Huguenin, M.T. Klein, *Ind. Eng. Chem., Prod. Res. Dev.* 24 (1985) 166.
- [9] G.V. Assche, A.V. Hemelrijck, H. Rahier, B.V. Mele, *Thermochim. Acta* 304(305) (1997) 317.
- [10] M. Reading, A. Luget, R. Wilson, *Thermochim. Acta* 238 (1994) 295.
- [11] E. Rabinowitch, *Trans. Faraday Soc.* 33 (1937) 1225.
- [12] C.W. Wise, W.D. Cook, A.A. Goodwin, *Polymer* 38 (1997) 3251.
- [13] M. Smoluchowski, *Phys. Chem.* 92 (1918) 129.
- [14] D. Heskamp, *Chem. Eng. Technol.* 21 (1998) 2.
- [15] N. Eckardt, H.J. Flammersheim, H.K. Cammenga, *J. Therm. Anal.* 52 (1998) 177.
- [16] H.J. Flammersheim, J. Opfermann, submitted to *Thermochim. Acta*.